

## A Dual-Polarized Fabry-Perot Cavity Antenna at Ka Band with Broadband and High Gain

Guan-Nan Tan, Xue-Xia Yang<sup>\*</sup>, Hai-Gao Xue, and Zhong-Liang Lu

**Abstract**—A broadband Fabry-Perot cavity antenna (FPCA) operates at Ka band with high gain and dual-polarization is reported. The proposed antenna employed a double-sided complementary-circular partially reflective surface (PRS) to enhance the directivity bandwidth. A square patch coupled by two orthogonal slots and fed by two microstrip lines was applied as the primary feed to achieve dual-polarization operation. To further improve the impedance bandwidth and directivity, a series of metal vias were suggested to surround the primary patch. This FPCA design was verified by the measurements. The experimental results show that the common impedance bandwidth of the two ports for the reflection coefficient ( $S_{11}$ ) below  $-10$  dB is 2.5 GHz from 34 GHz to 36.5 GHz (7.1%), which covers the common 3 dB gain bandwidth of the two ports. At the center frequency of 35 GHz, the measured peak gains at the two orthogonal ports are 16.1 dBi and 15.1 dBi, respectively. The isolation between the two ports is higher than 30 dB within the bandwidth.

### 1. INTRODUCTION

The millimeter-wave systems not only have high data-rate and small size, but also provide an access to the less crowded spectrum. They have been used in the local area networks, personal area networks, cellular communication, wireless power transmission systems, medical imaging and so on [1, 2]. In millimeter-wave bands, there are “windows” at 35 GHz, 94 GHz and 135 GHz. The atmospheric attenuations at these frequencies are low. In order to enhance the accessibility and capability of the millimeter-wave systems, antennas with polarization diversity and high gain have become more and more necessary. Microstrip antennas are preferable owing to their low profile, low cost and easy integration with the active devices. Large microstrip arrays have been succeeded at the normal microwave bands for high gain. However, the losses caused by the feeding network of microstrip array are high at millimeter-wave bands, which limit the antenna gain.

The partially reflecting sheet arrays were firstly introduced to antenna design by Trentini in 1956 [3], and then referred to as “Fabry-Perot cavity antennas (FPCAs)” by Feresidis and Vardaxoglou [4]. FPCAs provide several advantages of low complexity feeding network, high gain, and compatibility with the printed circuit board (PCB) process [5]. It is a good candidate in designing millimeter-wave antennas, but the 3 dB directivity bandwidths in literatures for millimeter-wave antennas were very narrow [6–9]. Patch antenna was used as the primary feed for several FPCAs at 60 GHz in [6]. The gains varied between 15.5 dB and 23.5 dB while the 3 dB directivity bandwidths were all less than 0.6%. A Fabry-Perot resonator antenna fed by an L-Probe was presented at 25.8 GHz in [8]. The antenna had a  $-10$  dB impedance bandwidth of 5% and a gain bandwidth of about 4% with the maximum gain of 11.1 dBi. In [9], a planar Fabry-Perot antenna operating at 44 GHz was proposed. The gain was 14 dBi, and the directivity bandwidth was only about 1%.

---

*Received 5 November 2015, Accepted 14 December 2015, Scheduled 22 December 2015*

<sup>\*</sup> Corresponding author: Xue-Xia Yang (yang.xx@shu.edu.cn).

The authors are with the Shanghai University, Shanghai, China.

In order to enhance the directivity bandwidth, some approaches have been developed. A simple way was decreasing the Q-factor by reducing the reflectivity of the PRS [10, 11]. However, the antenna gain would decrease obviously. The other way was employing antenna array as the primary feed [10, 12], but a complex feeding network would bring in loss and the gain improvement was very limited, especially in millimeter-wave. In [4], Feresidis and Vardaxoglou noted that a wide directivity bandwidth could be obtained if the gradient of reflection phase over the operation band was positive. Based on this principle, some kinds of designs have been introduced [13, 14]. In [13], three PRS layers were used, but the structure is thicker than  $1.4\lambda_0$  and complex to realize. In [14], using the rectangular-shape complementary PRS with low reflectivity to enhance the 3 dB directivity bandwidth at X band, but the maximum gain is only 13.8 dBi. In addition, the reflection performance of the rectangular-shape PRS designed isn't center symmetric, and would cause a problem when dealing with different polarized waves. For dual-polarization applications, some dual-polarized FPCAs have been designed [15–17]. In [15, 16], two separate primary patches were used to realize the dual-polarization characteristic, but that increases the complexity of the antennas. In [17], a dual circular polarization FPCA was proposed using the 3 dB-coupler, while the peak simulated realized gain was only 5.8 dBi.

In this paper, a broadband FPCA with high gain and dual-polarization operation at Ka band is presented. An orthogonal-slots-coupled patch antenna was used as the dual-polarized primary element. The complementary circular shape PRS was designed to enhance the directivity bandwidth at all incident wave directions. By surrounding the feed patch with a series of metal vias, the impedance bandwidth and the gain was improved further. A prototype was fabricated and measured to validate the design. The proposed antenna has a simple and low profile structure and low cost, which can be applied in many millimeter-wave systems.

## 2. ANTENNA DESIGN AND ANALYSIS

### 2.1. Antenna Design

The structure of the proposed FPCA is shown in Fig. 1. The antenna has three substrate layers, layers 1, 2 and 3 and one air layer. Layer 1 is the substrate of Rogers 3006 with the relative dielectric constant of 6.15 and the loss tangent of 0.0025. Layers 2 and 3 are all Rogers 5880 with the relative dielectric constant of 2.2 and the loss tangent of 0.0009. The thicknesses of the three layers were  $h_1$ ,  $h_2$  and  $h_3$ , respectively. The primary patch antenna is located on layers 1 and 2. The PRS was printed on the double side of layer 3, with the distance of  $h_c$  to the upper side of the primary antenna. All design models are implemented with the full-wave EM software HFSS.

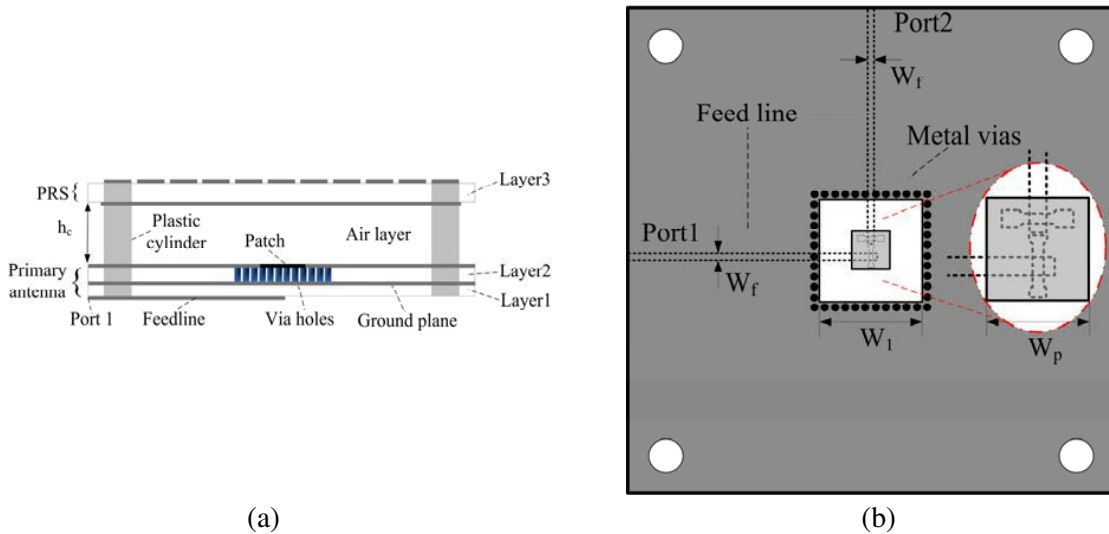


**Figure 1.** Structure of the proposed FPCA: (a) side view and (b) details of the primary antenna.

The details of the primary antenna are shown in Fig. 1(b). A patch antenna was printed on the top side of substrate layer 2. In order to realize dual-polarization operations at the same frequency, the square patch was placed at the center of the cavity and coupled by two orthogonal slots etched on ground plane. The two slots were placed centrally and perpendicularly to each other to improve the isolation between the two ports. Two  $50\ \Omega$  microstrip lines were placed on the bottom side of layer 1 to feed the primary antenna. In order to further improve the bandwidth and the gain, a series of metal vias were inserted around the patch with a distance larger than  $\lambda_g/4$ , which will be illustrated by simulation in the following subsection.

According to the early work of Trentini [3], the optical ray model can be used to theoretically explain the mechanism of the FPCA. With the multiple reflection of the wave emitted by the antenna, resonance would be achieved when the reflected waves are in phase after one cavity roundtrip. Thus, a highly directive beam can be obtained at the designed frequency. The resonance condition of this FPCA can be written by

$$\varphi_R - \pi - 4\pi h_c/\lambda_0 = 2N\pi, \quad N = 0, \pm 1, \pm 2 \quad (1)$$

where  $h_c$  is the height of the cavity,  $\varphi_R$  the reflection phase of the PRS and  $\lambda_0$  the free space wavelength. The cavity height  $h_c$  shown in Fig. 1 can be calculated from Eq. (1). However, the resonance condition presented in Eq. (1) is based on the analysis of plane wave excitations. For the proposed antenna, the wave is radiated by the patch antenna so the optimal cavity height should be found from the full wave simulation. Moreover, we can conclude from Eq. (1) that if  $\varphi_R$  were to increase linearly with the frequency, the phase variation of the PRS would compensate for the frequency variation of the cavity, which would lead to a wider bandwidth [4]. Assuming the size of the PRS to be infinite, the increased directivity of the FPCA can be calculate by [4]

$$D_{inc} = 10 \times \log \frac{1 + R}{1 - R} \quad (2)$$

where  $D_{inc}$  is the increased directivity comparing with the primary antenna, and  $R$  is the reflection magnitude of the PRS.

According to Eq. (2), in order to realize high directivity, the PRS with high reflection magnitude should be desired. The geometrical model of the proposed high reflectivity PRS is shown in Fig. 2(a). One unit cell was composed of two complementary circular structures. The circular patch with diameter  $D_p$  was printed on the upper side of the substrate layer 3 and the circular aperture with diameter  $D_a$  on the bottom side. The whole PRS array was composed of  $11 \times 11$  resonant cells separated by a distance  $P$ . The primary patch was placed at the center of the cavity and the EM fields were evanescent in the radial directions. The EM fields were very week at the edge of the cavity so the four corner cells were removed for further fixtures.

Master and slave boundaries for one unit were used to simulate the reflection performance of the PRS periodic array. The simulated reflection characteristics for different polarized plane waves of  $0^\circ$ ,  $22.5^\circ$  and  $45^\circ$  are shown in Fig. 3. It is found that the reflection performances are almost the same for different polarized waves. The minimum magnitude of the reflection coefficient for  $0^\circ$  polarization

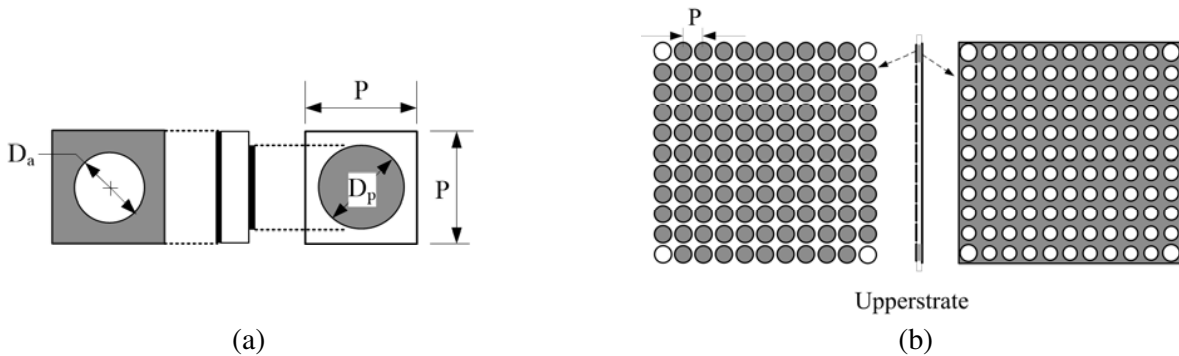


**Figure 2.** Geometrical model of PRS: (a) one unit cell and (b) whole unit cell array.

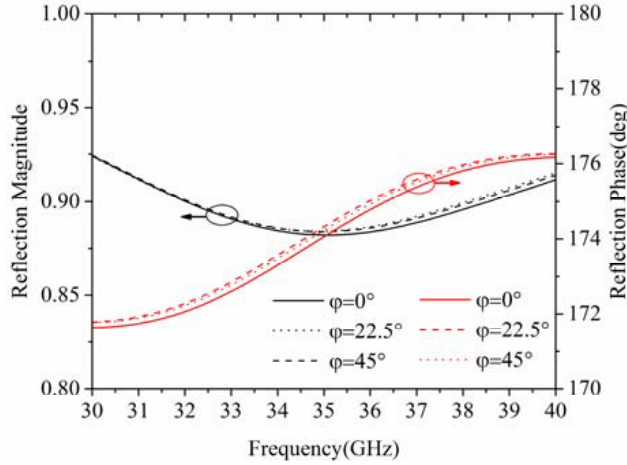


**Figure 3.** Simulated reflection characteristics of PRS.

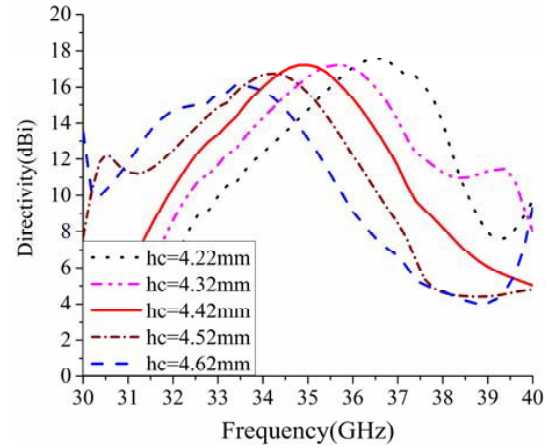


**Figure 4.** Simulated gain of port1 for varying  $h_c$ .

reaches 0.88 at the center frequency of 35 GHz. Moreover, the reflection phase increases linearly with the frequency from 34 GHz to 36 GHz. According to Eq. (1), a broadband directivity can be expected within the bandwidth. The designed PRS can be used in dual-polarization and circular polarization due to its characteristic of polarization insensitivity.

**2.2. Antenna Analysis**

By combining the suspended PRS layer with the primary antenna, the complementary FPCA was designed and analyzed. The initial value of cavity height  $h_c$  was 4.22 mm calculated from (1). Fig. 4 shows the parameter study of  $h_c$  at port 1. It can be observed that the cavity height has a great impact on the resonant frequency. With  $h_c$  increasing from 4.22 mm to 4.62 mm, the resonant frequency decreases from 36.6 GHz to 33.4 GHz. For the designed frequency 35 GHz, the directivity reaches the maximum when  $h_c$  is 4.42 mm.

The reflection waves of the PRS have a great influence on the impedance performance of the primary antenna. In this study, metal vias shown in Fig. 1(b) were inserted to minimize the influence and improve the bandwidth. The simulated reflection coefficient with and without metal vias around the patch are shown in Fig. 5. With the metal vias, the impedance bandwidth ( $S_{11} < -10$  dB) is 9.7%

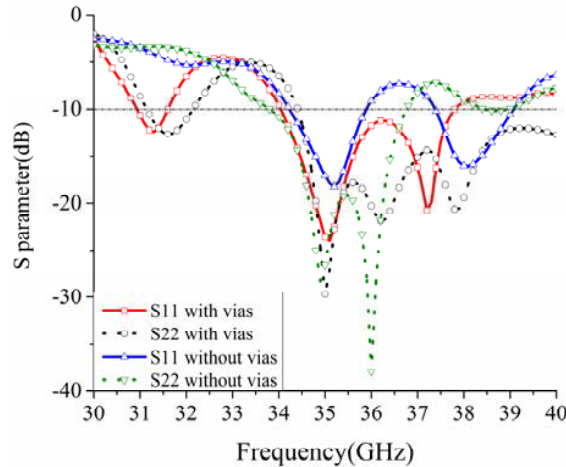


**Figure 5.** Reflection coefficient of the antenna.

ranging from 34.4 GHz to 37.8 GHz. But without the metal vias, the impedance bandwidth is only 4.6% ranging from 34.2 GHz to 35.8 GHz. It can be observed that the impedance bandwidth of the antenna with metal vias has been enhanced obviously. Meanwhile, the metal vias make the reflection waves of the ground plane uniformity and increase the directivity by 0.4 dB at 35 GHz.

### 3. FABRICATION AND MEASUREMENT

The antenna has been manufactured by using the standard PCB process, and the antenna pictures are shown in Fig. 6. The dimensions of the antenna are listed as follows:  $h_1 = 0.254$  mm,  $h_2 = h_3 = 0.508$  mm,  $h_c = 4.42$  mm,  $D_p = 2$  mm,  $D_a = 1.7$  mm,  $P = 2.4$  mm,  $W_f = 0.34$  mm,  $W_p = 2.23$  mm,  $W_1 = 6.6$  mm. The cavity height  $h_c$  is critical to the measurement. The PRS and primary antenna were separated by four plastic cylinders at the four corners of the substrate boards to form the air cavity, as shown in Fig. 6(c). The feed layer of the primary antenna has been extended to connect the end launch connector. The  $S$  parameter characteristics of the antenna were measured by the Agilent vector network analyzer of N5227A. The radiation patterns were measured in an anechoic chamber, which is based on the NSI 2000 antenna far-field measurement system designed by near-field Systems Incorporated.

The simulated and measured reflection coefficients and isolation of the fabricated antenna are depicted in Fig. 7. The simulated common impedance bandwidth of the reflection coefficient less than  $-10$  dB for the two polarization ports is about 10% at 35 GHz from 34.4 GHz to 37.9 GHz, while the measured one is about 7.1% at 35 GHz from 34 GHz to 36.5 GHz. The minor disagreement between the simulated and measured results mainly was due to the manufacture errors. The two polarization ports

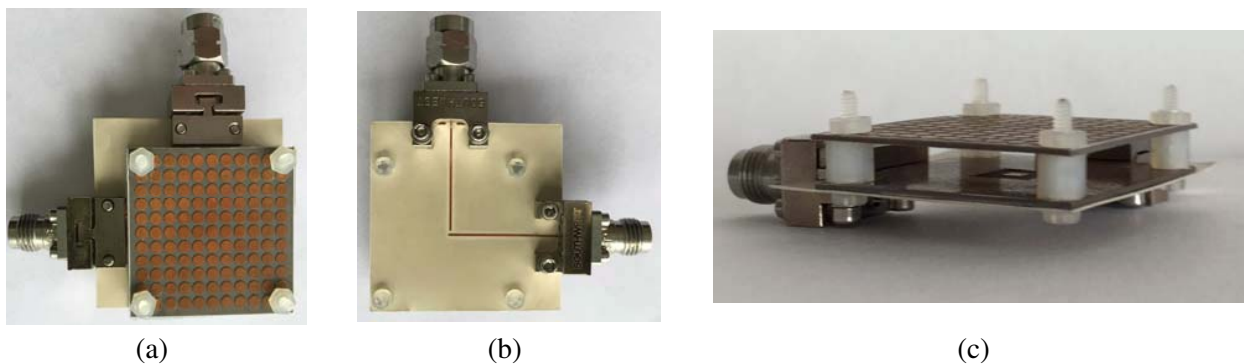


**Figure 6.** Photographs of the antenna prototype: (a) top view, (b) back view, (c) side view.

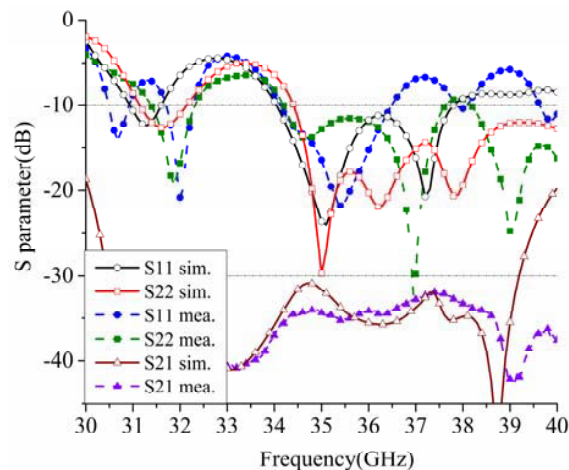


**Figure 7.** Simulated and measured  $S$  parameters.

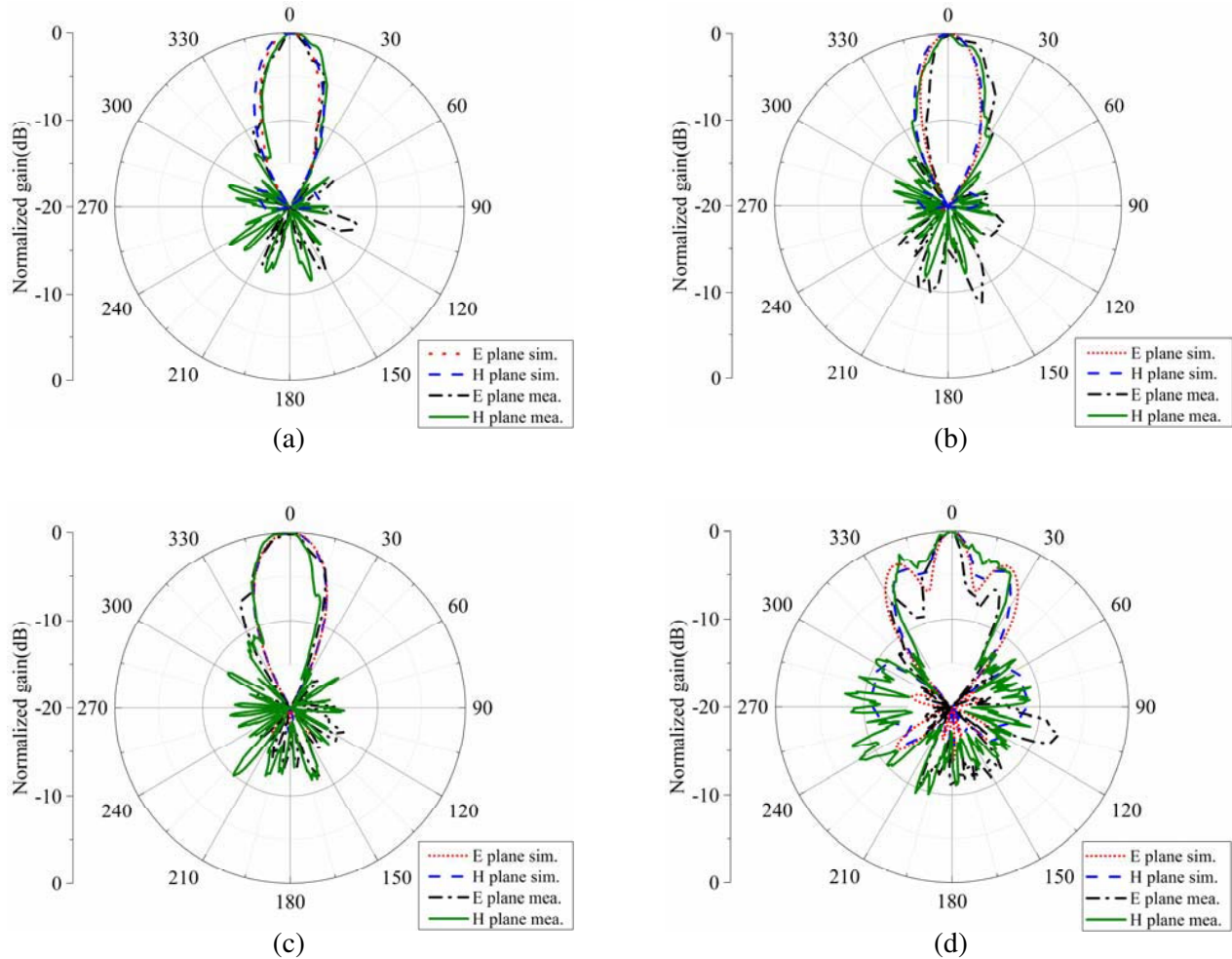


**Figure 8.** Simulated and measured radiation patterns: (a) port 1 @ 35 GHz, (b) port 2 @ 35 GHz, (c) port 1 @ 34 GHz, (d) port 1 @ 36.5 GHz.

have high isolation with the measured  $S_{21}$  within the bandwidth being lower than  $-30$  dB.

The  $H$ - and  $E$ -plane radiation patterns at 35 GHz for the two ports are shown in Figs. 8(a) and (b). The simulated front-to-back (F-B) ratios of port 1 and port 2 are 21 dB and 19 dB, respectively. The measured F-B ratios of the two ports are 20 dB and 15 dB. It can be found that port 1 exhibits higher F-B ratios than port 2. The main reason lies in the different arrangements of the coupling slots for the two ports. The coupling slot for port 1 is symmetric along the center vertical axis of the patch, while the coupling slot for port 2 is close to the edge. The measured side lobe levels (SLLs) of the two ports at 35 GHz are all lower than  $-13$  dB. The patterns of port 1 at 34 GHz and 36.5 GHz are plotted in Figs. 8(c) and (d). The patterns of port 2 are similar to those of port 1, which are not shown. The pattern at 34 GHz is similar to that at 35 GHz with low SLL, but at 36.5 GHz the SLL increases to  $-3$  dB due to the out-phase of the waves on the surface of PRS. The measured cross polarizations at these three frequencies are all lower than  $-20$  dB for the two polarization ports.

Figure 9 shows the gains versus the frequency for the two polarization ports. The measured peak gains for the two polarizations reached 16.1 dBi and 15.1 dBi at 35 GHz, respectively. The common 3 dB gain bandwidth of the two ports is 2.5 GHz from 34 GHz to 36.5 GHz, with the relative bandwidth of about 7.1% at the center frequency of 35 GHz. It can be seen that there are differences between the simulated and measured results. The differences are caused by two major reasons. The first one is the inaccurate loss-tangent values of the substrates provided by the datasheet which is obtained at 10 GHz. At millimeter-wave band, the values should be higher. In retro-simulation, the higher loss tangents

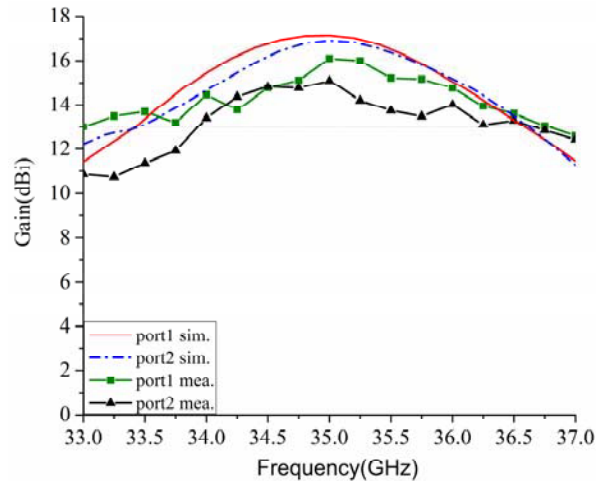


**Figure 9.** Simulated and measured gains.

values of 0.002 and 0.005 are chosen for Rogers 5880 and Rogers 3006, respectively. The simulated gain at 35 GHz decreases about 0.4 dB. The second reason between the simulated and the measured difference comes from the fabrication and measurement tolerances caused by the short wavelength of millimeter wave.

#### 4. CONCLUSION

A broadband FPCA with high gain and dual-polarization operation in Ka band has been proposed. The primary antenna is an orthogonal slots coupled patch. The broadband and high-gain characteristics have been achieved by the designed high reflectivity PRS with positive reflection phase gradient combining with the surrounding metal vias. The simulated and measured results verified the design. The measured common bandwidth of 3 dB gain and  $S_{11}$  less than  $-10$  dB of the two ports is 7.1% from 34 GHz to 36.5 GHz at the center frequency of 35 GHz. The peak gains are 16.1 dBi and 15.1 dBi for the two polarizations. And the isolation between the two-polarization port is higher than 30 dB within the bandwidth. The proposed PCB FPCA has a simple and low profile structure, which is easy to be integrated with other circuits. It can be applied in millimeter-wave communication and wireless power transmission systems. Moreover, the circular polarization operation for the antenna can be realized easily if the two ports are fed by the same amplitude and  $90^\circ$  phase difference because of the polarization insensitive characteristic of the proposed PRS.

#### ACKNOWLEDGMENT

This work is supported by the National Natural Science Foundation of China under Grant No. 61271062.

#### REFERENCES

1. Valliappan, N., A. Lozano, and R. W. Heath, "Antenna subset modulation for secure millimeter-wave wireless communication," *IEEE Trans. Commun.*, Vol. 61, No. 8, 3231–3245, Aug. 2013.
2. Shinohara, N., "Recent wireless power transmission via microwave and millimeter-wave in Japan," *2012 42nd European Microwave Conference (EuMC)*, 1347–1350, Amsterdam, Netherlands, Oct. 2012.
3. Trentini, G. V., "Partially reflecting sheet arrays," *IRE Trans. Antennas Propag.*, Vol. 4, No. 4, 666–671, Oct. 1956.
4. Feresidis, A. P. and J. C. Vardaxoglou, "High gain planar antenna using optimised partially reflective surfaces," *IEE Proc. — Microw. Antennas Propag.*, Vol. 148, No. 6, 345–350, Dec. 2001.

5. Costa, F. and A. Monorchio, "Design of subwavelength tunable and steerable Fabry-Perot/leaky wave antennas," *Progress In Electromagnetics Research*, Vol. 111, 467–481, 2011.
6. Sauleau, R., P. Coquet, and T. Matsui, "Low-profile directive quasi-planar antennas based on millimetre wave Fabry-Perot cavities," *IEE Proc. — Microw. Antennas Propag.*, Vol. 150, No. 4, 274–278, Aug. 2003.
7. Lee, Y., X. Lu, Y. Hao, S. Yang, J. Evans, and C. G. Parini, "Low-profile directive millimeter-wave antennas using free-formed three-dimensional (3-D) electromagnetic bandgap structures," *IEEE Trans. Antennas Propag.*, Vol. 57, No. 10, 2893–2903, Oct. 2009.
8. Kai, L., D. Yong, and W. L. Kwok, "A new Fabry-Perot resonator antenna fed by an L-probe," *IEEE Trans. Antennas Propag.*, Vol. 60, No. 3, 1237–1244, Mar. 2012.
9. Hosseini, S. A., F. Capolino, and F. De Flaviis, "Q-band single-layer planar Fabry-Perot cavity antenna with single integrated-feed," *Progress In Electromagnetics Research C*, Vol. 52, 135–144, 2014.
10. Weily, A. R., K. P. Esselle, T. S. Bird, and B. C. Sanders, "Dual resonator 1-D EBG antenna with slot array feed for improved radiation bandwidth," *IET Microw. Antennas Propag.*, Vol. 1, No. 1, 198–203, Feb. 2007.
11. Alkhatib, R. and M. Drissi, "Improvement of bandwidth and efficiency for directive superstrate EBG antenna," *Electron. Lett.*, Vol. 43, No. 13, 702–703, Jun. 2007.
12. Leger, L., T. Monediere, and B. Jecko, "Enhancement of gain and radiation bandwidth for a planar 1-D EBG antenna," *IEEE Microwave Wireless Compon. Lett.*, Vol. 15, No. 9, 573–575, Sep. 2005.
13. Konstantinidis, K., A. P. Feresidis, and P. S. Hall, "Multilayer partially reflective surfaces for broadband Fabry-Perot cavity antennas," *IEEE Trans. Antennas Propag.*, Vol. 62, No. 7, 3474–3481, Jul. 2014.
14. Wang, N., Q. Liu, C. Wu, L. Talbi, Q. Zeng, and J. Xu, "Wideband Fabry-Perot resonator antenna with two complementary FSS layers," *IEEE Trans. Antennas Propag.*, Vol. 62, No. 5, 2463–2471, May 2014.
15. Wang, M., Q. Ye, W. Wu, and D.-G. Fang, "A dual-polarized Fabry-Perot resonator antenna," *IEEE Asia-Pacific Conference Antennas Propag. (APCAP)*, 31–32, Singapore, Aug. 2012.
16. Sabri, L., N. Amiri, and K. Forooghi, "Dual-band and dual-polarized SIW-fed microstrip patch antenna," *IEEE Antennas Wireless Propag. Lett.*, Vol. 13, 1605–1608, 2014.
17. Vaid, S. and A. Mittal, "A three layer circularly polarized resonant cavity antenna," *IEEE International Microwave and RF Conference (IMaRC)*, 45–48, Bangalore, Dec. 2014.